2023 IEEE/ACM International Conference on Advances in Social Networks Analysis and Mining (ASONAM)

Brain network similarity using k-cores

Kazi Tabassum Ferdous
Dept. of Computer Science
University of Victoria
Victoria, Canada
Kferdous@uvic.ca

Sowmya Balasubramanian
Dept. of Computer Science
University of Victoria
Victoria, Canada
sowmyab@uvic.ca

Venkatesh Srinivasan
Dept. of Computer Science
University of Victoria
Victoria, Canada
srinivas@uvic.ca

Alex Thomo
Dept. of Computer Science
University of Victoria
Victoria, Canada
thomo@uvic.ca

***Abstract*—Autism Spectrum Disorder (ASD) is extensively studied by medical practitioners, health researchers, and educators. ASD symptoms appear in early childhood, within the first two years of life, but diagnosing it remains challenging due to its complex and diverse nature. Nevertheless, early diagnosis is crucial for effective intervention. Traditional methods rely on behavioral observations, while modern approaches involve applying machine learning (ML) to brain networks derived from fMRI scans. Limited explainability of these advanced techniques poses a significant challenge in gaining clinicians trust.**

This paper builds on recent works that design explainable approaches for ASD diagnosis from fMRI data preprocessed as graphs. Our research makes three key contributions. Firstly, we demonstrate that a simple approach based on viewing graphs as tables and using tabular data classifiers can achieve the same performance as state-of-art, explainable graph theoretic methods. Secondly, we provide evidence that by adding higher-order connectivity information as attributes does not improve their performance. Most importantly, we show why classification of brain networks is challenging by demonstrating the similarity between graphs belonging to individuals with ASD and those without, using a novel k-core based approach.

***Index Terms*—Autism Spectrum Disorder, ASD, ADHD, brain networks, fMRI, Hamming Distance, K-Cores, Jaccard Similarity**

I. Introduction

Autism Spectrum Disorder (ASD) is a developmental disorder caused by abnormal brain development, and encompasses a wide range of symptoms and severity levels, varying from mild to severe [1]. Individuals with ASD may have co-occurring conditions such as Attention Deficit Hyperactivity Disorder (ADHD), anxiety, or depression, which need to be addressed for comprehensive support [2]. They also face challenges in social interactions, exhibit repetitive behaviors and often have heightened sensitivity (hypersensitivity) or reduced sensitivity (hyposensitivity) to stimuli like light, touch, taste, or smell [3]. Despite this, they also possess remarkable strengths, such as visual thinking and problem-solving abilities.

ASONAM '23, November 6-9, 2023, Kusadasi, Turkey

ACM ISBN 979-8-4007-0409-3/23/11…$15.00
https://doi.org/10.1145/3625007.3627318

The exact cause of ASD is not fully understood, but research suggests that it results from a complex interplay of genetic and environmental factors [3]–[6]. ASD Symptoms typically emerge in early childhood affecting approximately 1 in 36 children, with boys being diagnosed four times higher than girls. It occurs across different racial, ethnic, and socioeconomic backgrounds without specific limitations [7]. Although there is no cure for ASD, early intervention, specialized services, and parental support improve a child's growth and development [8].

Diagnosing ASD requires a comprehensive specialist evaluation [9] and a detailed clinical assessment based on specific criteria outlined in diagnostic manuals like the DSM-5 [10]. Nevertheless, this traditional diagnostic approach lacks definitive laboratory tests and relies heavily on clinical judgment and behavioral observations. Therefore, it is important to employ reliable methods to improve ASD diagnosis for all ages.

The discovery of Functional MRI (fMRI), a modern brain imaging technique, has enabled researchers to identify and partition the brain into regions of interest (ROIs) based on their specific functions. By constructing a graph from a fMRI scan, with ROIs as vertices and edges representing the co-activation of these regions, researchers can employ graph classification techniques to effectively classify fMRI scans [11]. Several techniques have been proposed for general graph classification such as kernel methods [12], graph embeddings [13], and deep learning [14]. Metrics such as accuracy, precision, and recall are essential for evaluating any such classifier [15], and it has been shown that some of these methods can achieve impressively high scores for the various metrics.

However, a drawback of these techniques is their complexity, large number of parameters, and black-box nature making it challenging to understand their predictions. Recently, there is a growing focus on *explainability* within the AI domain [16], [17]. In critical sectors like healthcare, decision-makers are hesitant to adopt prediction models solely based on the high reported accuracy without comprehending their decision-making processes [18]. This cautious approach is especially crucial in healthcare, where *explainability* is vital for gaining the trust of medical practitioners [19].

In response to the need for explainability, Lanciano *et al.* [20] used *contrast subgraph* method for diagnosing ASD. The goal is to find subgraphs in brain connectivity data that display dense connections among individuals with ASD while

being sparse in neurotypical individuals, or vice versa. This approach aims to create an interpretable classification method revealing unique brain connectivity patterns in individuals with ASD. However, computing contrast subgraphs is complex and computationally intensive. In a recent study, Enns *et al.* [21] proposed a simpler *discriminative edges method*, which identifies the most important edges or connections that help distinguish individuals with ASD from neurotypical individuals. As shown in [21], both these methods obtained a mean accuracy of 60% on larger datasets of individuals with ASD. In light of these results, Enns *et al.* [21] poses the following question: Can brain imaging data lead to more accurate ASD diagnoses while maintaining explainability? If not, can we determine the reasons behind this limitation?

In our research, we seek to address this question by exploring an alternative pathway for explainable ASD diagnosis methods, complementing the findings of Lanciano *et al.* [20] and Enns *et al.* [21]. Our work views graphs as tables and focuses on demonstrating the effectiveness of simple and explainable tabular ML methods as alternatives to the graph techniques utilized in prior studies (e.g., [20], [21]). Furthermore, with the goal of improving the accuracy of our method, we explore the possibility of adding higher-order information as attributes to aid classification. While the methods we propose are simple and explainable, we observe that they did not achieve high accuracy though they matched the performance of the previous methods. Therefore, we investigate the potential barriers that hinder the achievement of strong performance metrics, aiming to provide insights into the question raised by [21]. Our main contributions are as follows:

1) Converting the brain network data into a tabular format and using explainable classifiers yield comparable results to graph-theoretic techniques used in prior works.
2) Incorporating higher-order connectivity patterns, the number of triangles in a node's neighbourhood, as attributes does not improve the classifier performance.
3) Studying similarities between brain networks of individuals with and without ASD, using similarity measures such as Jaccard similarity of k-cores and Hamming distance reveals the underlying barriers to ASD prediction.

II. Related Work

Over the years, there has been extensive research on the classification of ASD [22]–[27] using fMRI data. Several studies have explored diverse approaches to address this problem.

The traditional approach involves utilizing behavioral and family history information for ASD diagnosis. Misman *et al.* [28] have claimed impressive accuracy rates of up to 99% by employing Deep Neural Networks (DNNs) on ASD datasets that incorporate comprehensive behavioral and family history data. In an effort to improve the accessibility of these diagnosis techniques, Abbas *et al.* [29] developed mobile applications that coupled with machine learning techniques, show potential in aiding ASD diagnosis. However, it is important to note that relying solely on behavioral information may not provide an early and accurate diagnosis, as behavioral symptoms associated with ASD may not manifest until later in a child's development. Therefore, alternative methods focusing on biologically-based markers derived from fMRI scans are being explored.

Machine learning approaches have been widely employed in ASD classification using fMRI data [30], [31]. Researchers have utilized correlation matrices and deep learning models to achieve accurate classifications. For example, Liu *et al.* [30] have used Extra Trees algorithm to select relevant features from correlation matrices derived from fMRI data, resulting in an accuracy of 72% on the ABIDE dataset. Deep Learning models, such as Dense Neural Networks (DNNs), have also shown promise in achieving high accuracy of 88%, often surpassing classical machine learning models [32]. Feature selection techniques, such as sparse auto-encoders, have been employed to enhance classification performance and obtain accuracies above 90% [14].

However, it is important to consider the limitations of studies conducted on small datasets, as they may overfit the models and limit their generalizability to new datasets. Additionally, there is ongoing research to strike a balance between model performance and interpretability, as deep learning models are often considered "black-box" classifiers. Efforts are being made to develop explainable classification methods [16], [17], [33], allowing researchers and neuroscientists to gain insights and trust the predictions made by these models. These methods, such as [34], often involve deriving explanations for the model's decisions, such as SHAP values.

The present study is inspired by the work of Lanciano *et al.* [20]. They prioritized interpretable and simple features to aid neuroscientists' understanding, rather than solely aiming for high accuracy. In a similar vein, Coupette *et al.* [35] developed an algorithm to identify characteristic subgraphs with common and contrasting structures in graph groups, and illustrated their technique using brain networks from adolescents in the ABIDE dataset. Finally, Enns *et al.* [21] proposed the discriminative edges method with the goal of identifying a set of important edges that can separate the two classes. All these studies aim to uncover meaningful patterns in brain networks to enhance our understanding of ASD.

III. Datasets and Methods

In this section, we will first describe the datasets we use and the preprocessing steps involved in generating brain networks. Then, we will outline the methodologies employed for the classification and comparison of these brain networks.

A. Dataset Description

1) ASD Dataset: The study described in Section IV-A utilizes the ASD dataset obtained from Lanciano *et al.* [20] (https://github.com/tlancian/contrast-subgraph), which was originally released by the Autism Brain Imaging Data Exchange (ABIDE) project [36]. The dataset consists of neuroimaging data from 1112 individuals, comprising 573 Typically Developed (TD) individuals and 539 individuals diagnosed with Autism Spectrum Disorder (ASD). Typically

Developed (TD) individuals have normal brain function without neurological disorders whereas Autism Spectrum Disorder (ASD) individuals face autism-related challenges. Each individual in the dataset is represented by an undirected unweighted graph containing 116 vertices, where each vertex corresponds to a Region of Interest (ROI). The presence of an edge in the graph indicates strong a correlation in the activity between the two ROIs. The graphs are represented by an adjacency matrix of size 116×116.

Lanciano *et al.* created four distinct datasets from the original ABIDE source [36]. These datasets were curated by selecting individuals based on shared characteristics, such as age, gender, and scan conditions (e.g., eyes closed or male), as shown in Table I. Each of the dataset are divided into two classes namely TD and ASD and the dataset's description reflects shared phenotypic features among the observations. For instance, the "Children" dataset comprises individuals aged 9 years or younger, the "Adolescents" dataset includes individuals aged between 15 and 20 years, the "EyesClosed" dataset consists of individuals who underwent fMRI scans with their eyes closed, and the "Male" dataset exclusively includes male individuals.

Dataset	Description	TD	ASD
Children	Age ≤ 9	52	49
Adolescents	Age in [15,20]	121	116
EyesClosed	Eyes closed during scanning	158	136
Male	Male individuals	418	420

Table I
ASD DATASET - LANCIANO *et al.*

2) ADHD Dataset: In our experiments, as described in Section IV-B, we also used an ADHD dataset, which is another neurodevelopmental disorder impacting individuals of various age groups. ADHD is characterized by attention difficulties and impulsivity. Like ASD, the exact causes of ADHD remain unclear, and there is presently no cure for either condition. Nevertheless, treatments such as behavioral therapy and medication aid in symptom management and improving daily functioning [37]. By incorporating the ADHD dataset into our experiments, we gain valuable insights into the applicability of our techniques and results for ASD to other related disorders like ADHD.

Dataset	Description	TD	ADHD
ALL	ALL	330	190

Table II
ADHD DATASET - ABRATE *et al.*

This study uses the ADHD dataset from [38] (https://github.com/carlo-abrate/CounterfactualGraphs) which includes 330 individuals with typical development (TD) (normal brain function) and 190 individuals diagnosed with ADHD, as summarized in Table II. Similarly to the ASD dataset in Section III-A1, the ADHD dataset also portrays each individual with an undirected unweighted graph of 190 vertices, representing regions of interest (ROIs). The presence of an edge in the graph signifies a substantial correlation in the activity between the two ROIs, resulting in a adjacency matrix of size of 190×190.

For the parcellation of the brain, [20] used the AAL atlas for the ASD dataset ($|V| = 116$) and the authors of [38] used Craddock 200 (CC200) for the ADHD dataset $|V| = 190$).

B. Data Preprocessing

In our work, we use the ASD and ADHD graph datasets provided by [20], [38], without requiring any additional preprocessing. However, for completeness, we outline the preprocessing steps needed to convert fMRI scans into graphs.

Resting state fMRI is a neuroimaging technique that works by measuring the blood-oxygen-level-dependent (BOLD) signals in the brain. When a region of the brain becomes active, there is an increased demand for oxygenated blood to support the active neurons in that region. Therefore, the body responds by increasing the flow of oxygenated blood to that region. fMRI takes advantage of this body response to measure brain activity indirectly via BOLD signal intensities in different regions. The choice of the size of each region, and hence the number of such regions, is done using a brain atlas (AAL atlas, CC200). These regions are referred to as regions of interest (ROI). In summary, the output of an fMRI scan is a 3-dimensional image of the BOLD signal intensities in different ROIs of the brain measured over time.After obtaining the BOLD time series for each Region of Interest (ROI), the process of transforming it into graph data involves three essential steps:

1) **Analyze Patterns.** The communication pattern between different brain regions is examined by comparing their BOLD time series. The underlying premise is that the level of functional connections between two regions can be determined by assessing the correlation in their BOLD time series. The higher the correlation, the higher the functional connectedness.
2) **Calculate Pearson correlation coefficients (PCC).** Pairwise PCC is calculated between the BOLD time series for every pair of ROIs. This step yields a correlation matrix of size 116×116 (for ASD) or 190×190 (for ADHD), containing values in the range [-1, +1]. The correlation matrix acts as a weighted adjacency matrix, with ROIs as nodes and correlation coefficients as edge weights.
3) **Apply threshold.** Thresholding retains only the strongest connections, creating an undirected, unweighted graph like the ASD and ADHD datasets.

C. Classification Methods of Brain Networks

Graphs as tables. Recall that brain networks are simple, undirected graphs on 116 vertices in which each vertex has a unique id between 1 and 116. In order to convert a collection of such vertex-labeled brain networks into a table, we create a table with $\binom{116}{2} = 6670$ columns so that the table has one column for each possible edge in the graph. We can then

represent any brain network G as a binary vector, $T(G)$, of length 6670 such that a bit location labeled (i, j) stores a 1 if the edge (i, j) is present in G and 0 otherwise. We assume that the edges are listed in the lexicographic order.

Example. For the graph G shown in Fig. 1(a), the binary vector corresponding to G, $T(G)$, is $[101001110110101]$.

Tabular Classifiers. Transforming graph data into tables enables organized and structured analysis. Tables provide a tabular representation that allows for easier data manipulation, sorting, filtering, and statistical analysis compared to the graphical representation of the graph data. In this study, we utilize various tabular classifiers, including *SVM, Linear Regression, Random Forest, XGBoost, AdaBoost, and Perceptrons*. We evaluate performance using the four metrics: *Accuracy, Precision, Recall. and F1-score*. While all metrics are important, we present the top-3 classifiers selected based on their *accuracy* in Section IV. Our emphasis on accuracy aligns with previous works [20], [21].

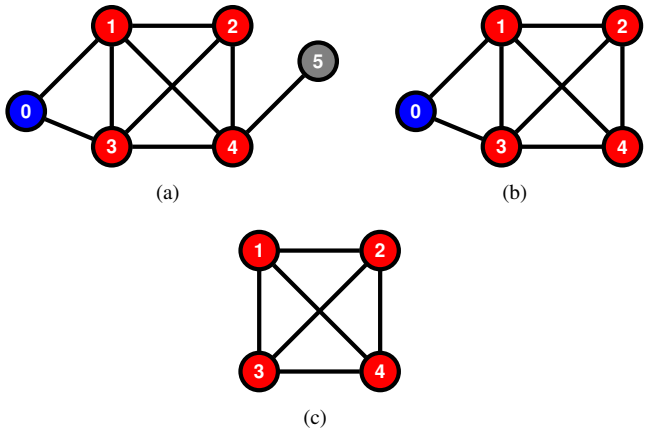

Figure 1. a) Graph $\mathcal{G}$, b) 2-core of $\mathcal{G}$, c) 3-core and Max-Core of $\mathcal{G}$.

Local Clustering Coefficient. Informally, the local clustering coefficient of a node i, C_i, in a graph measures the likelihood that the neighbours of i are also connected. Formally,

$$C_i = \frac{|\{(j,k) \mid j,k \in N_i, (j,k) \in E\}|}{\binom{|N_i|}{2}}$$

where N_i is the set of neighbours of node i. For each brain network, we will compute a tuple of size 116 containing the local clustering coefficient of its vertices.

Example. For the graph $\mathcal{G}$ in Fig. 1(a), the local clustering coefficient of vertex 0 is $C_0 = \frac{1}{\binom{2}{2}} = 1$ while $C_1 = \frac{1}{\binom{4}{2}} = 4/6$.

The local clustering coefficient is a measure introduced by Watts and Strogatz to study small world theory in social networks. As it measures interconnectedness among neighbors by counting triangles (a small graph pattern) centered at a node in essence, adding it as an additional attribute provides extra information about the graph and helps with ML tasks.

D. Comparison Methods of Brain Networks

To compare the collection of brain networks belonging to the two classes, ASD and TD, we use local clustering coefficient, Hamming distance, and k-core decomposition.

k-Core of a Graph. For a graph G and an integer k, $1 \leq k \leq n$, the k-core of G is the maximal subgraph H of G such that the induced degree of every vertex in H is at least k.

Note that, by the above definition, the $k+1$-core of G is a subset of the k-core of G, and hence the set of k-cores, $1 \leq k \leq n$, as k increases from 1 to n form a nested structure. This nested structure is referred to as k-core decomposition in the literature [39].

Example. Fig. 1(b) is the 2-core of the graph $\mathcal{G}$ in Fig. 1(a). In Fig. 1(b), each vertex is connected to at least 2 other vertices and it is also the maximal subgraph with that property. Note that 1-core of $\mathcal{G}$ is $\mathcal{G}$.

The study of k-cores offers valuable insights into the structure, resilience, and communities of complex networks, making it a popular topic in large-scale network analysis.

Max-Core of a Graph G**.** Let m, $1 \leq k \leq n$ be the integer such that the m-core of G is non-empty but its $m+1$-core is empty. If so, we refer to the m-core of G as its max-core.

Example. Fig. 1(c) is the 3-core of graph $\mathcal{G}$ in Fig. 1(a). In Fig. 1(c), each vertex is connected to at least 3 other vertices and it is also the maximal subgraph with that property such that this is the max-core as the 4-core of $\mathcal{G}$ is empty.

To compare max-cores of two different graphs G_1 and G_2, we use the notion of Jaccard similarity. Let V_1 and V_2 denote the set of vertices of G_1 and G_2.

Jaccard Similarity. Given two sets V_1 and V_2, we define their Jaccard similarity, $JS(V_1, V_2)$ as:

$$JS(V_1, V_2) = \frac{|V_1 \cap V_2|}{|V_1 \cup V_2|}$$

Example. Fig. 1(c) is the max-core G_1 of graph G and has vertices $V_1 = \{1, 2, 3, 4\}$. Lets assume G_2 is the max-core of another graph and has vertices $V_2 = \{1, 2, 7, 8, 9\}$, Jaccard similarity is computed as: $JS(V_1, V_2) = \frac{2}{7}$

Another notion that is useful to compare how close two graphs $\mathcal{G}$ and $\mathcal{G}'$ are based on their edges is the notion of Hamming distance.

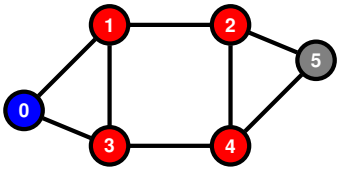

Figure 2. Graph $\mathcal{G}'$

Hamming Distance. Given two graphs $\mathcal{G}$ and $\mathcal{G}'$ on n vertices, the Hamming distance between $\mathcal{G}$ and $\mathcal{G}'$ is the minimum number of edge insertions and deletions needed to convert $\mathcal{G}$ to $\mathcal{G}'$. Equivalently, the Hamming distance between $\mathcal{G}$ and $\mathcal{G}'$ is the number of bit positions in which the two binary strings $T(\mathcal{G})$ and $T(\mathcal{G}')$ differ.

Example. Consider $\mathcal{G}$ and $\mathcal{G}'$ in Fig.1(a) and Fig.2. We need to add edges $(1, 4)$ and $(2, 3)$ and delete the edge $(2, 5)$ to convert $\mathcal{G}$ to $\mathcal{G}'$. Hence, the Hamming distance is 3.

IV. Results and Discussion

We now present the results we obtained from analyzing the ASD and ADHD datasets. The code and charts for our results can be found at https://github.com/sowbalas/HIBIBI2023.git.

A. Insights on ASD Dataset

The first research question of this study focuses on exploring the possibility of achieving explainability through a simple alternate pathway: the conversion of a graph into a table.

RQ1: How do well-known tabular classifiers perform on brain networks in tabular format?

By converting the graph dataset into tabular form, as described in Section III, we can employ a wide array of well-known tabular classifiers for flattened brain networks. Figure 3 presents our results (using ten-fold cross-validation), showing SVM (with a linear kernel) and Linear Regression (LR) consistently ranking among the top-3 classifiers across all four ASD datasets. These classifiers achieve a mean accuracy of close to 60% on larger datasets, like Male. The balanced nature of the ASD datasets sets the baseline accuracy at 50%.

The strong performance of SVM and LR classifiers, especially on larger datasets, indicate their potential significance in ASD diagnosis. Interestingly, these classifiers are highly explainable, and their accuracy closely matches that of sophisticated graph-theoretic methods from [21]. Enns *et al.* aimed to replicate Lanciano *et al.* work to comprehend the reported high accuracy. However, their results differed from the original study, demonstrating mean accuracies of 73.5% for Children, 60.8% for Adolescents, 58.5% for EyesClosed, and 59.3% for Male on the ASD dataset (Enns *et al.*, Table 4.2 in [21]). Our RQ1 results demonstrates a simple, alternate strategy to achieve explainability in ASD diagnosis using brain networks.

Our second question stems from the knowledge that graph classifiers can benefit from additional attributes beyond node and edge information as shown in [40].

RQ2: Can incorporating higher-order connectivity patterns, such as triangles, as attributes improve the performance of tabular classifiers?

To address this question, we created an augmented table by adding 116 new attributes, namely local clustering coefficients, to the table used for RQ1. However, the performance metrics (using ten-fold cross-validation) did not significantly improve. The top three classifiers on the ASD male dataset achieved a mean accuracy of 60%, as shown in Table III.

Accuracy	SVM	LR	NN
RQ2-Augmented table	0.60	0.60	0.60
RQ2-Clustering Coeff. only	0.55	0.55	0.54

Table III
RQ2 Top-3 Classifiers : ASD Male Dataset

In a related experiment, we further explored the classifiers performance when provided solely with higher order connectivity patterns. For this purpose, we created a tabular dataset with each row representing a brain network and 116 columns containing the local clustering coefficients of the nodes within the brain network. Table III displays the top three classifiers results in this scenario. SVM and LR, the most successful classifiers, achieved a lower mean accuracy of 55%.

To summarize, our findings for RQ1 and RQ2 reveal that tabular classifiers achieve a mean accuracy of around 60%. Despite attempting to enhance performance by incorporating higher-order information, such as local clustering coefficients, we did not observe notable improvements. This leads us to question whether there is a fundamental reason underlying this phenomenon. We further explore this inquiry through the concept of similarity measures.

RQ3: Can we provide evidence showing that the two classes of networks (ASD and TD) are quite similar?

We explore the presence of similarities between ASD and TD networks, through Hamming distance and Jaccard similarity of k-cores. The first approach, Hamming distance, focuses on edge-based similarity, while the second approach, Jaccard Similarity, centers on vertex-based similarity [41], [42].

Similarity based on Hamming distance.

Our first approach examines the similarity between the two categories of brain networks (TD and ASD) using the Hamming distance metric. We consider datasets from RQ1, where each brain network is represented as a binary string of length 6670. Each bit in the string represents a possible edge, with its value indicating the presence or absence of that edge. The Hamming distance between two brain networks is the minimum number of edge flips required to transform one network into the other, as defined in Section III-D.

Algorithm 1 Similarity based on Hamming distance

1: **Input**: A Dataset $D = \{G_1, G_2, \ldots, G_m\}$ consisting of two classes, ASD and TD files
2: **Output**: f_{ASD} and f_{TD} (the fraction of good ASD and TD files based on Hamming distance)
3: for each $G_i \in D$ do
4: $class \leftarrow class(G_i)$
5: $k \leftarrow \arg\min_{i \neq j} HD(G_i, G_j)$
6: **if** G_k is in the same class as G_i **then**
7: $count_{class}$++; $good_{class}$++
8: **else**
9: $count_{class}$++
10: **end if**
11: **return** $good_{ASD}/count_{ASD}$ and $good_{TD}/count_{TD}$

For each of the four datasets, we do the following (See Algorithm 1): For each brain network G_i in the dataset D containing ASD and TD files, we compute its Hamming distance to every other brain network G_j, $i \neq j$, in D. Using this information, we identify the brain network G_k that is closest to G_i in terms of Hamming distance (Lines 3 to 5 of Algorithm 1). That is, the brain network G_k requires the fewest number of edge additions and deletions to convert to

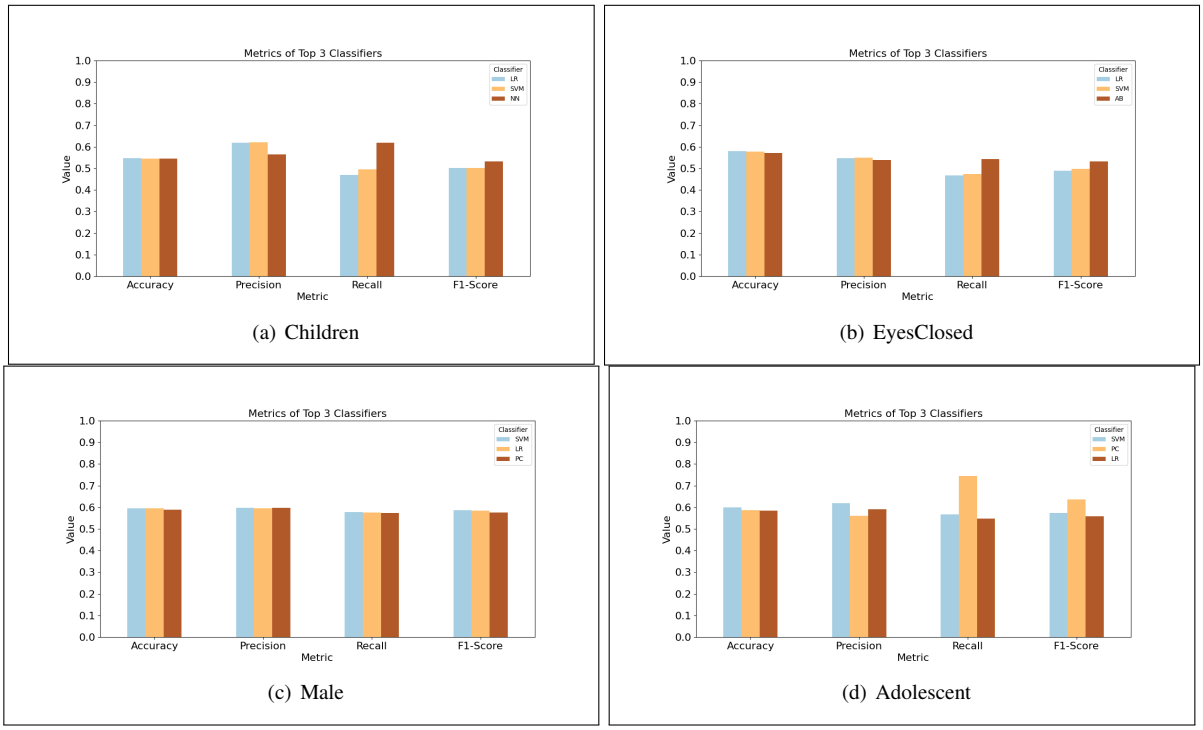

Figure 3. RQ1 - Performance Metrics of Top-3 Classfiers

G_i. G_i is a *good file* if G_k is in the same class as G_i and *bad file* if G_k is not in the same class as G_i (Lines 6 to 10).

As shown in Figure 4, in the Adolescent dataset, we observed that both the ASD and TD classes have approximately 40% of good files (in green), indicating that around 60% are bad files (in red). This finding is significant since it demonstrates that for the majority of brain networks, the most similar network belongs to the opposite class, not its own. Similar results across the other three datasets reinforce the conclusion that the widely used similarity measure fails to effectively distinguish between the two classes.

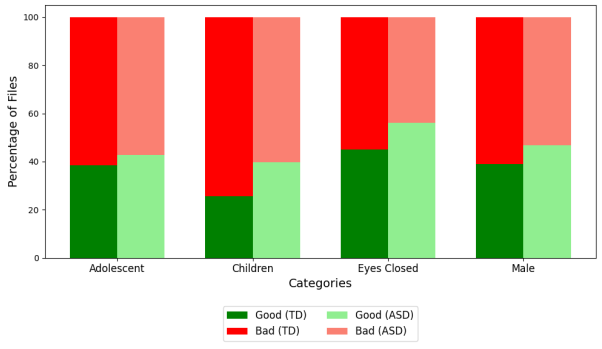

Figure 4. ASD Dataset: % of good and bad files using Hamming Distance

Jaccard Similarity based on k-cores.

Our approach involves employing the k-core as a "glocal" similarity measure, which combines aspects of both local and global metrics. This approach overcomes limitations found in traditional local (e.g., Hamming distance) and global (e.g., random walk-based) measures. Notably, prior research has recognized the importance of such glocal similarity measures, as discussed in [41], [42].

More specifically, we use the max-core of a brain network, as described in Section III-D. The primary objective is to assess whether the max-core of a given brain network resembles that of a typical ASD network or a TD network, using the Jaccard similarity metric. The max-core of a brain network comprises a set of ROIs where each ROI's time series exhibits strong correlations with at least k other ROIs. However, it's worth noting that computing the max-core is computationally intensive compared to the Hamming distance metric. To address this computational challenge, we have devised a more efficient procedure, drawing inspiration from ideas presented in [20] (see Algorithm 2).

1) Given a dataset, we partition the ASD files in that dataset into two sets, S_{ASD} and T_{ASD} using a 80:20 split. Similarly, we partition the TD files into two sets, S_{TD} and T_{TD} using a 80:20 split (Line 3 of Algorithm 2).
2) Using the files in S_{ASD}, we create a single graph, SG_{ASD}, that we call the ASD summary graph. This graph is a graph on 116 vertices. It contains an edge (i, j) if and only if more than 75% of the graphs in S_{ASD} contain that edge. Similarly, we create the TD summary graph SG_{TD} (Line 4).
3) We compute the max cores of the two summary graphs, SG_{ASD} and SG_{TD} (Line 5).
4) Now, for each file in T_{ASD}, we compute its max-core

Algorithm 2 Jaccard similarity of Max-Core

1: **Input**: A Dataset $D = \{G_1, G_2, \ldots, G_m\}$ consisting of two classes, ASD and TD files
2: **Output**: f_{ASD} and f_{TD} (the fraction of good ASD and TD files based on Jaccard similarity of max-core)
3: Partition D into four sets S_{ASD}, T_{ASD}, S_{TD}, and T_{TD} using 80:20 split.
4: Compute SG_{ASD} and SG_{TD} using 75% threshold.
5: Compute their max-cores, MC_{ASD} and MC_{TD}
6: for each $G_i \in T_{ASD}$ do
7: Compute max-core MC_i of G_i
8: **if** $JS(MC_i, MC_{ASD}) > JS(MC_i, MC_{TD})$ **then**
9: $count_{ASD}$++; $good_{ASD}$++
10: **else**
11: $count_{ASD}$++
12: **end if**
13: for each $G_i \in T_{TD}$ do
14: Compute max-core MC_i of G_i
15: **if** $JS(MC_i, MC_{TD}) > JS(MC_i, MC_{ASD})$ **then**
16: $count_{TD}$++; $good_{TD}$++
17: **else**
18: $count_{TD}$++
19: **end if**
20: **return** $good_{ASD}/count_{ASD}$ and $good_{TD}/count_{TD}$

and check if it closer to the max-core of SG_{ASD} or the max-core of SG_{TD} using Jaccard similarity. We say that it is *good* if it is closer to the max-core of SG_{ASD} and *bad* otherwise. Compute the percentage of good ASD files (Lines 6-12).

5) Repeat the previous step for TD files (Lines 13-19).

Figure 5 illustrates the results of our approach, representing mean percentages over ten runs. Taking the Adolescent dataset as an example, we observed that both the ASD and TD classes have approximately 40% and 60% of good files (displayed in green), respectively. This implies that the percentage of bad files is approximately 60% and 40% for ASD and TD, respectively. The noteworthy aspect of this observation is that for nearly half of the brain networks, the most similar network based on max-core comes from the opposite class, not its own. We found similar results for the other three datasets as well. This finding suggests that the Jaccard similarity of max-cores fails to differentiate between the two classes effectively.

To summarize, the results obtained using the two approaches in RQ3 provide robust and persuasive evidence of a high degree of similarity between the graphs in the two categories: ASD and TD. This explains the challenges faced by our classification methods and graph theoretic techniques used in prior research (e.g., contrast subgraph or discriminative edges method) in achieving strong performance metrics.

Run-time. All experiments were run on a Windows machine with Intel i5 CPU and 8 GB RAM. We report here the run times of our algorithms for RQ3. On the largest dataset (Male), a run of Algorithm 1 took 110 minutes to finish and on the smallest (Children), it took 75 seconds. This is because Algorithm 1 computes the Hamming distance between every pair of brain networks in the dataset. Algorithm 2 was much faster and required only 92 seconds on the Male dataset and 16 seconds on the Children dataset for one run as it only compared the max-core of 20% of the networks with the two summaries computed from the rest. A more detailed run-time analysis is deferred to the full version of the paper.

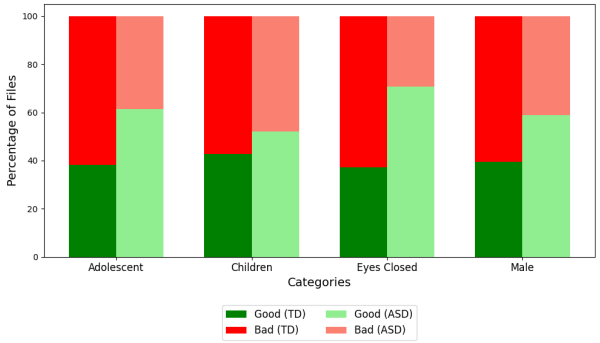

Figure 5. ASD Dataset: % of good and bad files using Jaccard Similarity

B. Insights on ADHD Dataset

Our results for RQ1-RQ3 prompt the question of whether these outcomes are specific to the ASD dataset we studied. We are interested in understanding whether our approach could yield different results when applied to a dataset focused on a different but closely related health condition. To address this, we conduct an investigation using the ADHD dataset and apply the same methodology as described for the ASD dataet. We noted that, for this dataset, the top-3 tabular classifiers achieved an accuracy of 63% for RQ1 and did not perform much better than the baseline classifier.

When we compared the two classes, ADHD and TD, for RQ3, the average percentages of good files remains around 50% for Jaccard similarity and 35% for Hamming distance, (refer to Figure 6). These results indicate that our findings for ASD datasets extend to the ADHD dataset as well.

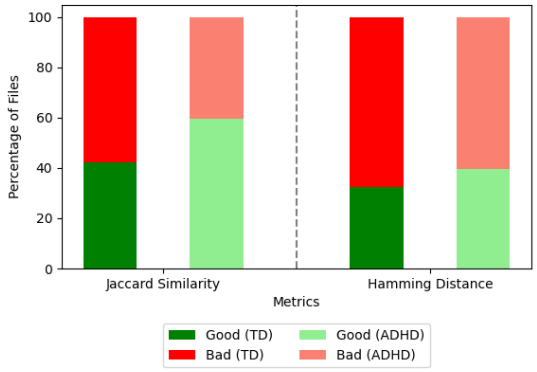

Figure 6. ADHD Dataset: % of good and bad files using Jaccard Similarity & Hamming Distance

V. Conclusions

Early diagnosis of ASD or other related developmental disorders is crucial for providing individuals with the medical services and social support needed. Given our lack of understanding about its causes and cure, new techniques are needed to improve diagnosis. This work investigates the potential of biomarkers obtained from fMRI scans in the diagnosis of ASD and ADHD. It shows that tabular classifiers can achieve performance comparable to the best-known graph-theoretic methods that are explainable. At the same time, it demonstrates the challenges in classifying brain networks using two similarity measures, Hamming distance and Jaccard similarity of max-cores on available datasets. Our results imply further research using larger fMRI datasets could alleviate the current challenges and thus lead to further progress.

References

[1] G. Fischbach, "Leo kanner's 1943 paper on autism," https://www.spectrumnews.org/opinion/viewpoint/leo-kanners-1943-paper-on-autism/.

[2] W. H. O. R. O. for the Eastern Mediterranean, "Autism spectrum disorders," Technical documents, 2019.

[3] M. B. Lauritsen, "Autism spectrum disorders," *European child & adolescent psychiatry*, vol. 22, pp. 37–42, 2013.

[4] P. G. Enticott, H. A. Kennedy, N. J. Rinehart, B. J. Tonge, J. L. Bradshaw, J. R. Taffe, Z. J. Daskalakis, and P. B. Fitzgerald, "Mirror neuron activity associated with social impairments but not age in autism spectrum disorder," *Biological psychiatry*, vol. 71(5), pp. 427–433, 2012.

[5] L. M. Hernandez, J. D. Rudie, S. A. Green, S. Bookheimer, and M. Dapretto, "Neural signatures of autism spectrum disorders: insights into brain network dynamics," *Neuropsychopharmacology (New York, N.Y.)*, vol. 40, no. 1, pp. 171–189, 2015.

[6] L. de la Torre-Ubieta, H. Won, J. L. Stein, and D. H. Geschwind, "Advancing the understanding of autism disease mechanisms through genetics," *Nature medicine*, vol. 22, no. 4, pp. 345–361, 2016.

[7] CDC, "Cdc," https://www.cdc.gov/ncbddd/autism/data.html.

[8] S. L. Hyman, S. E. Levy, S. M. Myers, D. Z. Kuo, S. Apkon, L. F. Davidson, K. A. Ellerbeck, J. E. Foster, G. H. Noritz, M. O. Leppert *et al.*, "Identification, evaluation, and management of children with autism spectrum disorder," *Pediatrics*, vol. 145, no. 1, 2020.

[9] S. B. Mukherjee, "Autism spectrum disorders—diagnosis and management," *The Indian Journal of Pediatrics*, vol. 84, pp. 307–314, 2017.

[10] APA, *Diagnostic and statistical manual of mental disorders : DSM-5™.*, 5th ed. Washington, DC ;: American Psychiatric Publishing, a division of American Psychiatric Association, 2013.

[11] E. Bullmore and O. Sporns, "Complex brain networks: graph theoretical analysis of structural and functional systems," *Nature reviews neuroscience*, vol. 10, no. 3, pp. 186–198, 2009.

[12] P. Shervashidze, Nino andf Schweitzer, E. J. Van Leeuwen, K. Mehlhorn, and K. M. Borgwardt, "Weisfeiler-lehman graph kernels." *Journal of Machine Learning Research*, vol. 12, no. 9, 2011.

[13] L. Gutiérrez-Gómez and J.-C. Delvenne, "Unsupervised network embeddings with node identity awareness," *Applied Network Science*, vol. 4, no. 1, pp. 1–21, 2019.

[14] Y. Kong, J. Gao, Y. Xu, Y. Pan, J. Wang, and J. Liu, "Classification of autism spectrum disorder by combining brain connectivity and deep neural network classifier," *Neurocomputing*, vol. 324, pp. 63–68, 2019.

[15] C. Elkan, "Evaluating classifiers," *UC San Diego*, 2012.

[16] A. Hassan, R. Sulaiman, M. Abdulgabber, and H. Kahtan, "Towards user-centric explanations for explainable models: A review," *J. of Information System and Technology Management*, vol. 6, pp. 36–50, 2021.

[17] P. Linardatos, V. Papastefanopoulos, and S. Kotsiantis, "Explainable ai: A review of machine learning interpretability methods," *Entropy*, vol. 23(1), 2021.

[18] O. Asan, A. E. Bayrak, and A. Choudhury, "Artificial intelligence and human trust in healthcare: Focus on clinicians," *J Med Internet Res*, vol. 22, no. 6, p. e15154, Jun 2020.

[19] S. Tonekaboni, S. Joshi, M. D. McCradden, and A. Goldenberg, "What clinicians want: contextualizing explainable machine learning for clinical end use," in *Machine learning for healthcare conference*. PMLR, 2019, pp. 359–380.

[20] T. Lanciano, F. Bonchi, and A. Gionis, "Explainable classification of brain networks via contrast subgraphs," in *KDD*, 2020, pp. 3308–3318.

[21] K. Enns, V. Srinivasan, and A. Thomo, "Identifying autism spectrum disorder using brain networks: Challenges and insights," *Proc. of Int. Conf. on Information, Intelligence, Systems and Applications (IISA)*, 2023. [Online]. Available: https://dspace.library.uvic.ca/handle/1828/14937

[22] C. P. Santana, E. A. de Carvalho, I. D. Rodrigues, G. S. Bastos, A. D. de Souza, and L. L. de Brito, "rs-fmri and machine learning for asd diagnosis: a systematic review and meta-analysis," *Scientific reports*, vol. 12, no. 1, pp. 6030–6030, 2022.

[23] M. R. Arbabshirani, S. Plis, J. Sui, and V. D. Calhoun, "Single subject prediction of brain disorders in neuroimaging: Promises and pitfalls," *NeuroImage (Orlando, Fla.)*, vol. 145, no. Pt B, pp. 137–165, 2017.

[24] C.-W. Woo, L. J. Chang, M. A. Lindquist, and T. D. Wager, "Building better biomarkers: brain models in translational neuroimaging," *Nature neuroscience*, vol. 20, no. 3, pp. 365–377, 2017.

[25] J. O. Maximo, E. J. Cadena, and R. K. Kana, "The implications of brain connectivity in the neuropsychology of autism," *Neuropsychology review*, vol. 24, no. 1, pp. 16–31, 2014.

[26] H. S. Nogay and H. Adeli, "Machine learning (ml) for the diagnosis of autism spectrum disorder (asd) using brain imaging," *Reviews in the neurosciences*, vol. 31, no. 8, pp. 825–841, 2020.

[27] M. Khodatars, A. Shoeibi, D. Sadeghi, N. Ghaasemi, M. Jafari, P. Moridian, A. Khadem, R. Alizadehsani, A. Zare, Y. Kong, A. Khosravi, S. Nahavandi, S. Hussain, U. R. Acharya, and M. Berk, "Deep learning for neuroimaging-based diagnosis and rehabilitation of autism spectrum disorder: A review," *Computers in biology and medicine*, vol. 139, pp. 104 949–104 949, 2021.

[28] M. F. Misman, A. A. Samah, F. A. Ezudin, H. A. Majid, Z. A. Shah, H. Hashim, and M. Harun, "Classification of adults with autism spectrum disorder using deep neural network," in *AiDAS'19*, pp. 29–34.

[29] H. Abbas, F. Garberson, S. Liu-Mayo, E. Glover, and D. P. Wall, "Multi-modular ai approach to streamline autism diagnosis in young children," *Scientific reports*, vol. 10, no. 1, pp. 1–8, 2020.

[30] Y. Liu, L. Xu, J. Li, J. Yu, and X. Yu, "Attentional connectivity-based prediction of autism using heterogeneous rs-fmri data from cc200 atlas," *Experimental neurobiology*, vol. 29, no. 1, pp. 27–37, 2020.

[31] R. M. Thomas, S. Gallo, L. Cerliani, P. Zhutovsky, A. El-Gazzar, and G. van Wingen, "Classifying autism spectrum disorder using the temporal statistics of resting-state functional mri data with 3d convolutional neural networks," *Frontiers in Psychiatry*, vol. 11, 2020.

[32] F. Z. Subah, K. Deb, P. K. Dhar, and T. Koshiba, "A deep learning approach to predict autism spectrum disorder using multisite resting-state fmri," *Applied Sciences*, vol. 11, no. 8, 2021.

[33] G. Yang, Q. Ye, and J. Xia, "Unbox the black-box for the medical explainable ai via multi-modal and multi-centre data fusion: A mini-review, two showcases and beyond," *Information Fusion*, vol. 77, pp. 29–52, 2022.

[34] A. Perotti, P. Bajardi, F. Bonchi, and A. Panisson, "Graphshap: Motif-based explanations for black-box graph classifiers," *arXiv preprint arXiv:2202.08815*, 2022.

[35] C. Coupette, S. Dalleiger, and J. Vreeken, "Differentially describing groups of graphs," *Proc. of AAAI Conference on Artificial Intelligence*, vol. 36, no. 4, pp. 3959–3967, Jun. 2022.

[36] S. M. Adirana Di Martino, "Abide," http://fcon_1000.projects.nitrc.org/indi/abide/abide_I.html.

[37] NHS, "Nhs," https://www.nhs.uk/conditions/attention-deficit-hyperactivity-disorder-adhd/.

[38] C. Abrate and F. Bonchi, "Counterfactual graphs for explainable classification of brain networks," in *KDD*, 2021, pp. 2495–2504.

[39] W. Khaouid, M. Barsky, V. Srinivasan, and A. Thomo, "K-core decomposition of large networks on a single pc," *PVLDB*, vol. 9(1), pp. 13–23, 2015.

[40] N. Pržulj, "Biological network comparison using graphlet degree distribution," *Bioinformatics*, vol. 23, no. 2, pp. e177–e183, 2007.

[41] G. Jurman, R. Visintainer, M. Filosi, S. Riccadonna, and C. Furlanello, "The him glocal metric and kernel for network comparison and classification," in *DSAA*, 2015, pp. 1–10.

[42] G. Nikolentzos, P. Meladianos, S. Limnios, and M. Vazirgiannis, "A degeneracy framework for graph similarity." in *IJCAI*, 2018, pp. 2595–2601.